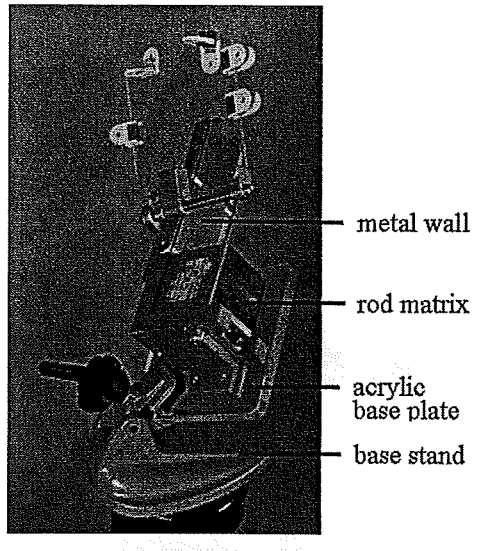

Fig. 2. A photograph of the compensator assembling unit. Each compensator rod was manually piled up to make 11 by 11 rod matrix.

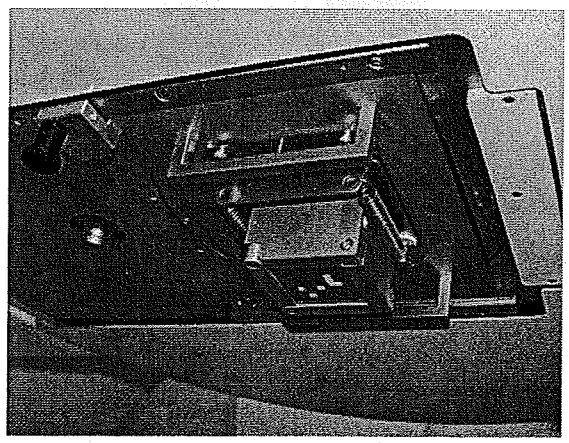

Fig. 3. A photograph of the assembled compensator attached to the gantry head.

the bottom plane of the compensator rods was 530.5 mm. The projected field size of the 11 by 11 rod matrix on the isocenter (center of gantry rotation) plane was approximately 104 mm × 104 mm. Although most of previous compensators required the MLC to shield outside the tumor target region, the proposed compensator would require only block collimators to avoid radiation on and outside the compensator metal wall because the X-ray transmission through the 50 mm tungsten rod was considered sufficiently small. In order to minimize the inter-rod leakage on the central axis, the rods were firmly compressed by the metal wall and were aligned to a half-offset position with respect to the central axis. 5000 MU (Monitor Unit) was delivered to an X-ray film (EDR2, Kodak) through an 11 by 11 rod matrix having a tungsten thickness of 50 mm to evaluate the inter-rod leakage and the transmission.

Subsequently, tungsten compound plates (Heavy Metal, Sumitomo Electric) each having a thickness of 5 mm were piled up to provide 0, 5, 15, 25, 35, 50 mm thickness for determining the X-ray linear attenuation coefficient. The material property of the tungsten rod and the tungsten plate was identical. The X-ray transmission was measured by a Farmer type ion chamber (0.6 cm^3, PTW TN30013) as a function of the thickness of the tungsten compound. The ion chamber was placed

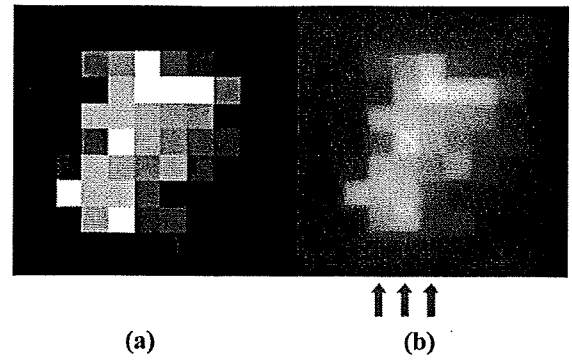

Fig. 4. (a) Simulated intensity map based on a simple exponential model. (b) Dose profile read by the film scanner.

at the depth of 100 mm solid water phantom, which coincided with the isocenter position. Another 100 mm solid water phantom was placed below the isocenter. A tray factor, when no rods were placed between the two 1-mm-thick acrylic plates in the compensator enclosure, was also measured. The calculation of the linear attenuation coefficient was repeated with three different field sizes of 30 mm × 30 mm, 50 mm × 50 mm, and 70 mm × 70 mm. The resulting attenuation coefficients were plotted as a function of the side length of the square field, and the linear attenuation coefficient without scattering effect was obtained by extrapolating the plot to field size zero.

After determining the linear attenuation coefficient of the tungsten compound for our 6 MV linac, each tungsten rod length was calculated according to the rule shown in Fig. 1(b). Then, a compensator was constructed to test intensity modulation capability. Another EDR2 film was positioned perpendicular to the beam axis on an isocenter plane with two 100 mm solid water phantoms above and below the film. After delivering 300 MU, the intensity modulated dose profiles on the film were measured by a film scanner (R-TECH, DD system) and compared to the intensity map calculated by the measured linear attenuation coefficient and the simple exponential model [5].

III. Results

Based on the measured tray factor of 0.979 and TMR (Tissue Maximum Ratio) of 0.7913 at 100-mm depth for a field size of 100 mm × 100 mm, the transmission through the 50 mm tungsten rod matrix was approximately 2.5% and the maximum leakage between rods was approximately 2.7% according to the film readings.

The semi-log plot of X-ray transmission was linear up to 50 mm tungsten length for each of the three different field sizes, and a linear attenuation coefficient of 0.0763 mm^{-1} was obtained. The lengths of the tungsten compound were determined as follows: 1.38, 2.92, 4.67, 6.69, 9.08, 12.01, 15.78, 21.09, 30.18, and 50.0 mm. Fig. 4(a) shows a simulated intensity map calculated from the exponential attenuation model with the measured linear attenuation coefficient. Fig. 4(b) shows measured dose distribution using the film. The vertical arrows indicate the scanning lines, and the scanned results are shown in the next figure.

Fig. 5(a)–(c) demonstrates relative dose distribution read by the film scanner. The step patterns show calculated intensity profiles using the measured linear attenuation coefficient and the exponential attenuation model.

IV. Discussion

Unlike the previous cubic-block-based compensator having a fixed height [13], the proposed rod matrix compensator can provide a con-

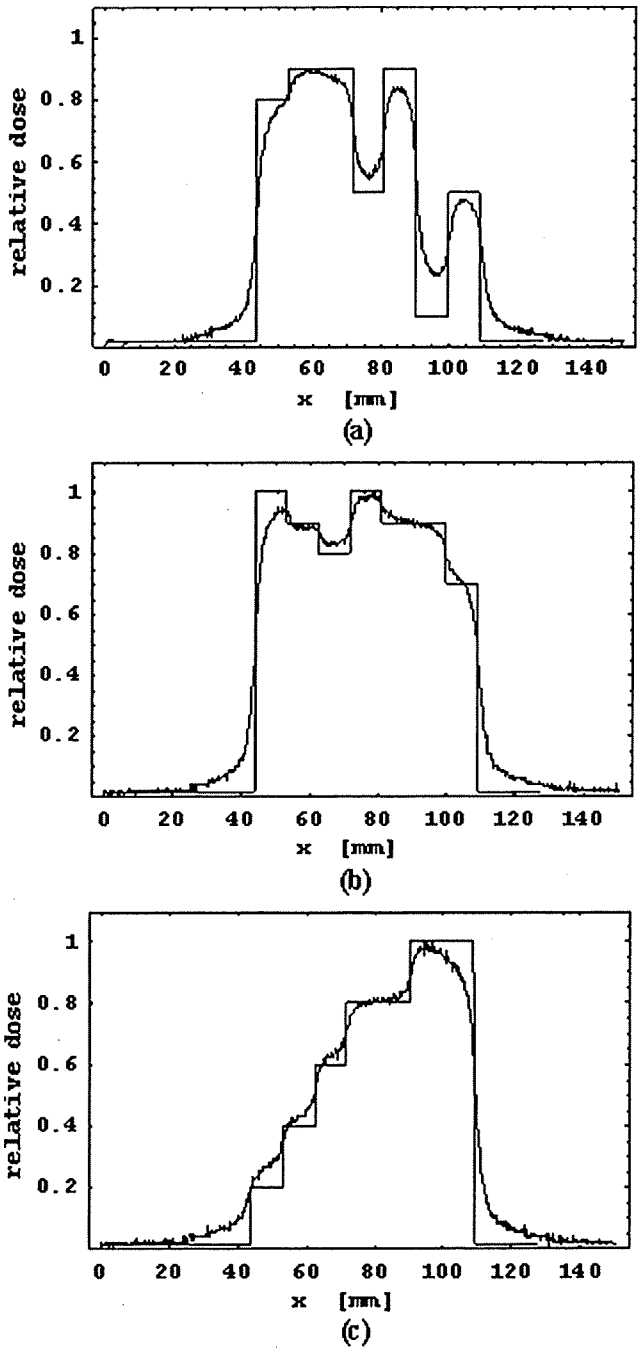

Fig. 5. (a)–(c) Relative dose distribution read by the film scanner. The scanned line positions correspond to the three vertical arrows in Fig. 4(b) from left to right in order. The step patterns show calculated intensity profiles using the measured linear attenuation coefficient and the exponential attenuation model.

stant incremental intensity step of 10% by optimizing each length of the tungsten portion. Another advantage of the rod matrix compensator is that a multileaf collimator is not required to shield outside the target region. This means that the rod matrix compensator allows a linac without MLC to perform IMRT. The previous cubic-block-based compensator employed a tungsten-dominant resin having a density of as low as 12 g/cm^3; and therefore, piled-up blocks of 50-mm height led to 10% transmission [13].

In Fig. 5(a) –(c), we see reasonable correspondence between dose measurement and intensity calculation. It is well known that an X-ray film containing silver has a significantly higher sensitivity at an X-ray energy below 100 keV due to photo electric effect. In addition, the beam energy is quickly degraded at the time of lateral scattering [14]. Consequently, the lateral scattering in the water phantom would be the cause of the significant discrepancies at the two low dose regions near the center of Fig. 5(a). A very similar result was also demonstrated and discussed in a reference [15] that may also support this speculation.

The proposed compensator can be used with a rotating mount means [12]. This combination minimizes human labor during treatment because several compensators can be exchanged automatically. A major disadvantage of the proposed compensator is that the maximum field size is limited to 11 cm × 11 cm when the compensator is placed at a distance of 50 cm from the source. However the proposed compensators are considered to be an effective tool for a small tumor treatment because delivery time is comparable to conventional open beam treatment. It should be noted that a small tumor needs to be positioned more accurately than a large tumor and more time-consuming MLC-based IMRT would increase the chance of organ movements during treatment.

In the meantime, Shirato reported that their fluoroscopic breathing-gated procedure led to excessive kV dose if used with MLC-based IMRT that requires longer treatment time [16]. The prolonged dose delivery may also have an undesirable radiobiological impact on IMRT treatment outcome [17]. It is, therefore, expected that these issues can be effectively solved by using a compensator-based IMRT. Compensator-based IMRT dose calculation using Pinnacle treatment planning system (Philips/ADAC) is under commissioning phase, and the three-dimensional dose verification with the proposed compensator will be reported in the near future.

REFERENCES

[1] A. Brahme, "Optimization of stationary and moving beam radiation therapy techniques," *Radiother. Oncol.*, vol. 12, pp. 129–140, 1988.
[2] P. J. Keall, H. Cattell, D. Pokhrel, S. Dieterich, K. H. Wong, M. J. Murphy, S. S. Vedam, K. Wijesooriya, and R. Mohan, "Geometric accuracy of a real-time target tracking system with dynamic multileaf collimator tracking system," *Int. J. Radiat. Oncol. Biol. Phys.*, vol. 65, pp. 1579–1584, 2006.
[3] S. Webb, "Motion effects in (intensity modulated) radiation therapy: A review," *Phys. Med. Biol.*, vol. 51, pp. R403–R425, 2006.
[4] F. Ellis, E. J. Hall, and R. Oliver, "A compensator for variations in tissue thickness for high energy beams," *Br. J. Radiol.*, vol. 32, pp. 421–422, 1959.
[5] A. Djordjevich, D. J. Bonham, E. M. A. Hussein, J. W. Andrew, and M. E. Hale, "Optimal design of radiation compensators," *Med. Phys.*, vol. 17, pp. 397–404, 1990.
[6] J. Stein, K. Hartwig, S. Levegrun, G. Zhang, K. Preiser, G. Rhein, J. Debus, and T. Bortfeld, "Intensity-modulated treatments: Compensators vs. multileaf modulation," in *Proc. XIIth ICCR*, Salt Lake City, UT, May 1997, pp. 338–341.
[7] S. B. Jiang and K. M. Ayyangar, "On compensator design for photon beam intensity-modulated conformal therapy," *Med. Phys.*, vol. 25, pp. 668–675, 1998.
[8] S. X. Chang, K. M. Deschesne, T. J. Cullip, S. A. Parker, and J. Earnhart, "A comparison of different intensity modulation treatment techniques for tangential breast irradiation," *Int. J. Radiat. Oncol. Biol. Phys.*, vol. 45, pp. 1305–1314, 1999.
[9] S. X. Chang, T. J. Cullip, and K. M. Deschesne, "Intensity modulation delivery techniques: Step & shoot MLC auto-sequence versus the use of a modulator," *Med. Phys.*, vol. 27, pp. 948–959, 2000.
[10] S. X. Chang, T. J. Cullip, K. M. Deschesne, E. P. Miller, and J. G. Rosenman, "Compensators: An alternative IMRT delivery technique," *J. Appl. Clin. Med. Phys.*, vol. 5, pp. 15–36, 2004.
[11] T. Xu, P. M. Shikhaliev, M. Al-Ghazi, and S. Molloi, "Reshapable physical modulator for intensity modulated radiation therapy," *Med. Phys.*, vol. 29, pp. 2222–2229, 2002.

[12] K. Yoda and Y. Aoki, "A multiportal compensator system for IMRT delivery," *Med. Phys.*, vol. 30, pp. 880–886, 2003.
[13] K. Nakagawa, N. Fukuhara, and H. Kawakami, "A packed building-block compensator (TETRIS-RT) and feasibility for IMRT delivery," *Med. Phys.*, vol. 32, pp. 2231–2235, 2005.
[14] S. E. Burch, K. J. Kearfott, J. H. Trueblood, W. C. Sheils, J. I. Yeo, and C. K. C. Wang, "A new approach to film dosimetry for high energy photon beams: Lateral scatter filtering," *Med. Phys.*, vol. 24, pp. 775–783, 1997.
[15] Å. Palm, A. S. Kirov, and T. LoSasso, "Predicting energy response of radiographic film in a 6 MV X-ray beam using Monte Carlo calculated fluence spectra and absorbed dose," *Med. Phys.*, vol. 31, pp. 3168–3178, 2004.
[16] H. Shirato, M. Oita, K. Fujita, Y. Watanabe, and K. Miyasaka, "Feasibility of synchronization of real-time tumor-tracking radiotherapy and intensity-modulated radiotherapy from viewpoint of excessive dose from fluoroscopy," *Int. J. Radiat. Oncol. Biol. Phys.*, vol. 60, pp. 335–341, 2004.
[17] J. Z. Wang, X. A. Li, W. D. D'Souza, and R. D. Stewart, "Impact of prolonged fraction delivery times on tumor control: A note of caution for intensity-modulated radiation therapy (IMRT)," *Int. J. Radiat. Oncol. Biol. Phys.*, vol. 57, pp. 543–552, 2003.